A STRUCTURAL ANALYSIS OF NERVE MYELIN

C. R. WORTHINGTON *and* A. E. BLAUROCK

From the Department of Physics and Biophysics Research Division, University of Michigan, Ann Arbor, Michigan 48104

ABSTRACT A structure analysis of the low-angle X-ray diffraction data from nerve myelin is described. The low-angle X-ray data are interpreted in terms of an electron density strip model which has five parameters, these refer to the dimensions of the membrane pair and their component electron densities. Three sets of low-angle X-ray data from peripheral nerve swollen in media of different electron densities are analyzed and membrane pair dimensions and component electron densities on an absolute scale are assigned. Membrane pair dimensions are given for a variety of peripheral nerve myelins and central nervous system myelins.

INTRODUCTION

The molecular organization of nerve myelin has been studied extensively by birefringence, X-ray diffraction, and electron microscopy. On the basis of these physical studies, together with a knowledge of its chemical composition, nerve myelin consists of concentric layers of lipo-protein spirally wrapped around the axon. The X-ray diffraction pattern of intact or live myelinated nerve shows a series of discrete low-angle X-ray reflections which are related to the radial packing of the concentric lipo-protein layers. The low-angle X-ray diffraction pattern of intact peripheral nerve myelin (Schmitt, Bear, and Palmer, 1941) shows the first five orders of a radial repeat distance of 170–185 A depending on the variety of nerve. The center-to-center layer distance is the radial repeating unit and each layer consists of two Schwann cell membranes. The low-angle X-ray diffraction pattern of intact central nervous system myelin (Finean, 1960) shows only two orders of diffraction but the first five orders of a radial repeat distance of 150–160 A depending on the variety of nerve have now been recorded (Blaurock and Worthington, 1969).

A structural interpretation of the low-angle X-ray diffraction data from nerve myelin can, in principle, lead to a set of precise model parameters. Various arrangements (Schmitt et al., 1941) and molecular models (Finean, 1953; Vandenheuvel, 1963) have been proposed for peripheral nerve myelin and these all contain some kind of bimolecular leaflet of lipid. The molecular models contain two bimolecular

leaflets of lipid per radial repeat, one for each Schwann cell membrane. Whether any of these models are correct, or not, is not yet known, because none of these models have been tested with the X-ray data. In view of the mode of formation of myelinated nerve (Geren, 1954; Robertson, 1964) it is reasonable to assume a center of symmetry within the radial repeating unit. This assumption of a center of symmetry considerably simplifies any structural analysis. In order to proceed with a structural analysis of the low-angle X-ray diffraction data, either of two approaches can be adopted; the model approach or the Fourier approach. Previous work has centered on the Fourier approach. On the basis of swelling phenomena of peripheral nerve myelin, Moody (1963) has given two sets of phases for the first five diffraction orders of intact peripheral nerve myelin whereas Finean and Burge (1963) have chosen one of these sets of phases and have computed a Fourier synthesis for intact frog and rat sciatic nerves. However, the interpretation of a low-resolution Fourier synthesis in terms of a model has its problems (Worthington, 1969) and the identification of certain features in the Fourier with molecular parameters of a particular model is certainly not rigorous.

In this paper we adopt the model approach and we use X-ray intensities corrected for cylindrical layering. The correction factors needed to convert the observed X-ray diffraction intensities to the modulus of the Fourier transform of the radial repeating unit have been described (Blaurock and Worthington, 1966).

It is easy to see why a direct application of the model approach to intact nerve is not likely to succeed unless a simple model comes to mind. In order to test any proposed model with the X-ray data the number of diffraction orders must exceed the number of model parameters (Worthington, 1969). The low-angle X-ray pattern of intact myelinated nerve generally shows with moderate exposure times only five orders of diffraction and hence the number of model parameters which can be derived is restricted. Consider a basic triple-layered model for the Schwann cell membrane, for instance, the model described by Worthington and Blaurock (1968). This model has five parameters and the prospects of determining meaningful model parameters from an analysis of the low-angle X-ray data from intact myelinated nerve are remote. However, the case of peripheral nerve myelin swollen in distilled water, hypotonic Ringer's solutions or sucrose solutions is different, for up to 13 orders have been recorded within the same angular range as the five orders from intact nerve myelin. Hence, direct application of the model approach to swollen nerve is not ruled out because of the limited number of diffraction orders, and there is good prospects of obtaining a set of fairly precise model parameters.

In the course of our analysis we examine a number of possible models in order to account for the low-angle X-ray data from swollen peripheral nerve myelin. A description of the chosen electron density model has been briefly reported elsewhere (Worthington and Blaurock, 1968). From an analysis of swollen nerve patterns obtained by immersing frog sciatic nerve in media of different electron densities, a value for the electron density of the swollen membrane pair is obtained. We describe com-

ponent electron densities within the membrane pair in terms of electrons/A^3. A talk on the electron density levels in peripheral nerve myelin has been presented (Worthington and Blaurock, 1969 *a*).

EXPERIMENTAL

The equipment and methods used in obtaining low-angle X-ray diffraction patterns of myelinated nerve and in measuring the integrated intensities have been previously described (Blaurock and Worthington, 1969). For the present paper the following description is given. X-ray films were measured using a low-power microscope. The X-ray reflections from nerve myelin obey Bragg's law $2d \sin \theta = h\lambda$ where d is the radial repeat distance and h is the diffraction order. The integrated intensities $I(h)$ were measured using a Joyce-Loebl microdensitometer model MK III C.

In this previous study we recorded low-angle X-ray diffraction patterns from a variety of myelinated nerves and, in particular, found that the first five diffraction orders from these patterns had a characteristic intensity variation. There are two intensity variations: one for peripheral nerve myelin and one for central nervous system myelin. The well known low-angle X-ray diffraction patterns from intact peripheral nerve myelin (Schmidt et al., 1941; Finean, 1960) show only the first five diffraction orders of the radial repeat distance. However, by using a low-angle X-ray camera with increased camera speed, higher diffraction orders can be recorded (Blaurock and Worthington, 1969), but only one of these higher orders ($h = 6$) is included in the present analysis. We have also described the first five orders of diffraction from intact central nervous system myelin and these five orders are used in the present analysis.

We examine low-angle X-ray data from live or intact nerves. Peripheral nerves include sciatic nerves from frog, rat and chicken. Central nervous system nerves include optic nerves from frog, rat, and chicken and frog spinal cord. The radial repeat distances and intensity variations for these nerves have been given and photographs of selected patterns from sciatic nerves of frog, rat, and chicken, and from an optic nerve of rat have been shown (Blaurock and Worthington, 1969).

In a study of the swelling behavior of peripheral nerve myelin we have identified three kinds of low-angle X-ray diffraction patterns (Worthington and Blaurock, 1969 *b*). These are the normal pattern from intact or live nerve, the swollen pattern from nerve immersed in distilled water, hypotonic Ringer's solution or in sucrose solutions and the subnormal pattern obtained as a result of adding salt solution to nerve preswollen in distilled water. These three kinds of low-angle X-ray diffraction patterns together with the specimen preparation procedures have been described in detail (Worthington and Blaurock, 1969 *b*). We examine the low-angle X-ray data from three swollen patterns obtained by immersing frog sciatic nerve in distilled water, 0.24 and 0.82 M sucrose solutions. We also examine the low-angle data from one subnormal pattern obtained by immersing frog sciatic nerve, which had been

previously swollen in distilled water, in 1 mM $CaCl_2$. Photographs of the swollen patterns of frog sciatic nerve in distilled water and in 0.24 M sucrose solution and a subnormal pattern of frog sciatic nerve (a different concentration of 2 mM $CaCl_2$ was used) have been shown (Worthington and Blaurock, 1969 *b*).

TREATMENT OF LOW-ANGLE X-RAY DATA

Before any structure analysis can proceed one first needs to obtain the modulus of the Fourier transform from the integrated intensity data $I(h)$. Let $t(x)$ represent the electron density distribution of the one-dimensional radial repeating unit and let $T(X)$ represent the corresponding Fourier transform, where x, X are real and reciprocal space coordinates (for example, see Blaurock and Worthington, 1966). We use the notation $J(h) = |T(h)|^2$. The relation between the integrated intensities $I(h)$ of nerve myelin and $J(h)$ is:

$$I(h) \alpha J(h)/h \qquad (1)$$

where α is the proportional sign (Blaurock and Worthington, 1966). Hence, a set of intensities, corrected for the cylindical layering, is obtained from the low-angle X-ray patterns but on a relative scale. Let $J_{obs}(h)$ describe this set of intensities. We use the notation $J(h) = J(0) + J'(h)$, $T(h) = T(0) + T'(h)$ where $J'(h) = |T'(h)|^2$ as we do not record the zero order reflection. In order to convert our set of intensities

TABLE I

RELATIVE INTENSITIES $J_{obs}(h)$ FOR PERIPHERAL NERVE MYELIN

h	f.s.*	r.s.‡	c.s.§	s.f.s. (1)‖	s.f.s.(2)¶	s.f.s. (3)**	s.n.f.s.‡‡
1	0.003	0.003	0.003	0.015	0.005	0.140	0.004
2	0.422	0.352	0.324	0	0.006	0.052	0.376
3	0.107	0.107	0.079	0.378	0.001	0.041	0.176
4	0.341	0.396	0.333	0.516	0.164	0.462	0.236
5	0.089	0.104	0.054	0.028	0.600	0.704	0.122
6	0.005	0.006	0.006	0.213	0.615	0.422	0
7				0.267	0.248	0.077	0.054
8				0.055	0.010	0.005	
9					0.096	0.089	
10					0.240	0.084	
11					0.210	0.021	
12					0.072		
13					0.006		

* f.s.—intact frog sciatic nerve, d = 171 A, X_o = 6/171 A^{-1}.
‡ r.s.—intact rat sciatic nerve, d = 176 A, X_o = 6/176 A^{-1}.
§ c.s.—intact chicken sciatic nerve, d = 182 A, X_o = 6/182 A^{-1}.
‖ s.f.s. (1)—swollen frog sciatic nerve, in distilled water, d = 252 A, X_o = 8/252 A^{-1}.
¶ s.f.s. (2)—swollen frog sciatic nerve, in 0.24 M sucrose, d = 388 A, X_o = 13/388 A^{-1}.
** s.f.s. (3)—swollen frog sciatic nerve, in 0.82 M sucrose, d = 359 A, X_o = 11/359 A^{-1}.
‡‡ s.n.f.s.—subnormal frog sciatic nerve, in 1 mM $CaCl_2$, d = 166 A, X_o = 7/166 A^{-1}.

TABLE II

RELATIVE INTENSITIES $J_{obs}(h)$ FOR CENTRAL NERVOUS SYSTEM MYELIN

h	f.o.*	r.o.‡	c.o.§	f.s.c.‖
1	0.011	0.005	0.005	0.011
2	0.620	0.628	0.653	0.626
3	0.039	0.014	0.028	0.032
4	0.318	0.281	0.228	0.308
5	0.012	0.036	0	0.023

* f.o.—Frog optic nerve, $d = 154$, A, $X_o = 5/154$ A^{-1}.
‡ r.o.—rat optic nerve, $d = 159$ A, $X_o = 5/159$ A^{-1}.
§ c.o.—chicken optic nerve, $d = 155$ A, $X_o = 5/155$ A^{-1}.
‖ f.s.c.—frog spinal cord, $d = 153$ A, $X_o = 5/153$ A^{-1}.

$J_{obs}(h)$ to an absolute scale we write $J'(h) = K J_{obs}(h)$ where K is the normalization constant. The intensity data $J_{obs}(h)$ for the various peripheral and central nervous system myelins together with their radial repeat distances and reciprocal space cut-off values are listed in Tables I and II.

COMPARISON OF DIFFERENT SETS OF INTENSITY DATA $J_{obs}(h)$

The swelling behavior of peripheral nerve myelin (Finean and Millington, 1957) suggests the possibility of experimentally obtaining a continuous intensity plot $J_{obs}(X)$, $X = h/d$ by varying the radial repeat distance d. Consider two swollen patterns which show different radial periods d_1 and d_2. Denote the two sets of intensity data $J_{obs}(h)$ as $J_1(h)$ and $J_2(h)$. Each set of intensity data can be converted to an absolute scale provided the normalization constant K is known. K can be evaluated in terms of a model to be described in the following section (see K for model (2 d) in Table III, Worthington, 1969). Thus, we can write

$$(2/d) \sum_{1}^{h} J'(h) = \Omega \qquad (2)$$

where Ω is dependent on the parameters of the membrane pair contained in the model, and $\Omega \approx 8pl(P - L)^2/w$. We note that Ω is not dependent on the radial repeat distance d or the fluid layer. Hence the relation

$$K(2/d) \sum_{1}^{h} J_{obs}(h) = \Omega \qquad (3a)$$

allows K to be found for each set of intensity data $J_{obs}(h)$.

However, if Ω is not known, then it is desirable to place each set of intensity data on the same relative scale. For instance, we want to convert $J_2(h)$ to the same relative scale as $J_1(h)$. Therefore, on the basis of the above theory we require to find a

factor k such that

$$k(2/d_2) \sum_{1}^{h} J_2(h) = (2/d_1) \sum_{1}^{h} J_1(h). \qquad (3b)$$

This is easily performed. We next examine the correctness of using this procedure in converting different sets of intensity data $J_{obs}(h)$ to the same relative scale.

Consider three sets of intensity data from nerve myelin swollen in sucrose solutions. One of the low-angle X-ray patterns is from frog sciatic nerve immersed in 0.24 M sucrose solution; this pattern shows 13 diffraction orders of d = 388 A. A detailed description of this pattern has been given previously and a reproduction of the pattern has been shown (Worthington and Blaurock, 1969 *b*). The other two low-angle X-ray patterns were also obtained from frog sciatic nerve in 0.24 M sucrose solution, but with either 4 mM KCl or 4 mM NaCl added to the sucrose solution; 10 diffraction orders of d = 326 A and 12 diffraction orders of d = 373 A were recorded respectively. The intensity data has been converted to the same relative scale by use of equation 3 *b*. Integrated intensities $I(h)$ have a range of 300:1 and the corrected intensities $J_{obs}(h)$ have a similar (but smaller) range. For convenience, in comparing

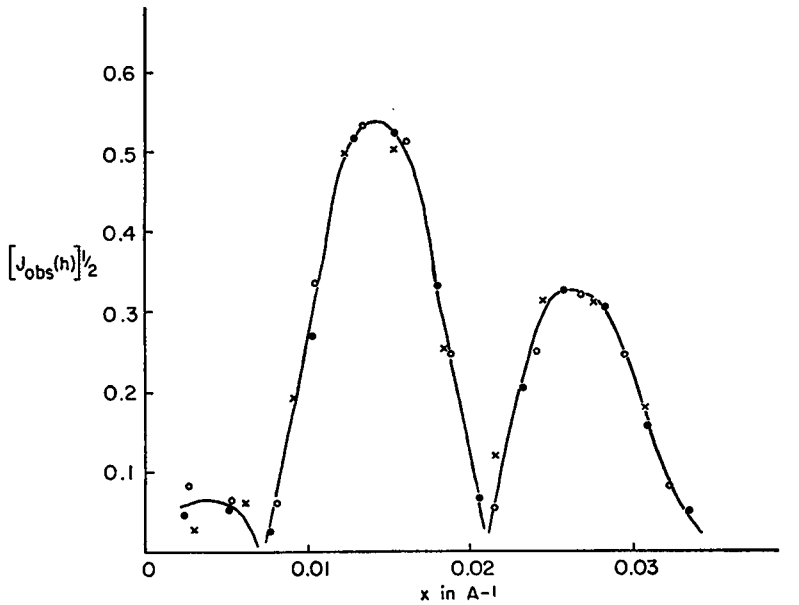

FIGURE 1 The modulus of the amplitude $[J_{obs}(h)]^{1/2}$ for three sets of low-angle X-ray data are plotted against X, the reciprocal space coordinate. The three sets of data have been put on the same relative scale using equation 3 *b*. The continuous curve is fitted by eye to the experimental points. (Solid circle) the 0.24 M sucrose data, d = 388 A; (open circle) the 0.2 M sucrose with 4 mM NaCl data, d = 373 A; (cross) the 0.24 M sucrose with 4 mM KCl data, d = 326 A.

different sets of intensity data we choose to construct curves using the modulus of amplitude $[J_{obs}(h)]^{1/2}$. The three sets of data are shown in Fig. 1. Each set of amplitude data $[J_{obs}(h)]^{1/2}$ lies on a continuous curve (with three minima), which can be drawn, as shown in Fig. 1.

Consider a further three sets of intensity data, two from frog sciatic nerve swollen in distilled water and the other one obtained from immersing frog sciatic nerve, which had been previously swollen in distilled water, in 1 mM $CaCl_2$ solution. The patterns from frog sciatic nerve in distilled water are as follows: eight diffraction orders of $d = 252$ A and ten diffraction orders of $d = 342$ A. The subnormal pattern is from sciatic nerve, preswollen in distilled water, but recorded after treatment with 1 mM $CaCl_2$ solution. This pattern shows the first seven orders of $d = 166$ A. These three patterns have been previously described, and photographs of the $d = 252$ A pattern and a very similar subnormal pattern obtained using 2 mM $CaCl_2$ solution have been published (Worthington and Blaurock, 1969 *b*). After using equation 3 *b* to convert the intensity data to the same relative scale, the three sets of data using amplitudes $[J_{obs}(h)]^{1/2}$ are plotted in Fig. 2. Each set of amplitude data lies on a continuous curve (with three minima), which can be drawn, as shown in Fig. 2.

The fact that three different sets of intensity data (we plot amplitudes) from frog sciatic nerve swollen in 0.24 M sucrose solutions with different radial repeat distance all lie on a continuous curve suggests that our procedure for converting each set of

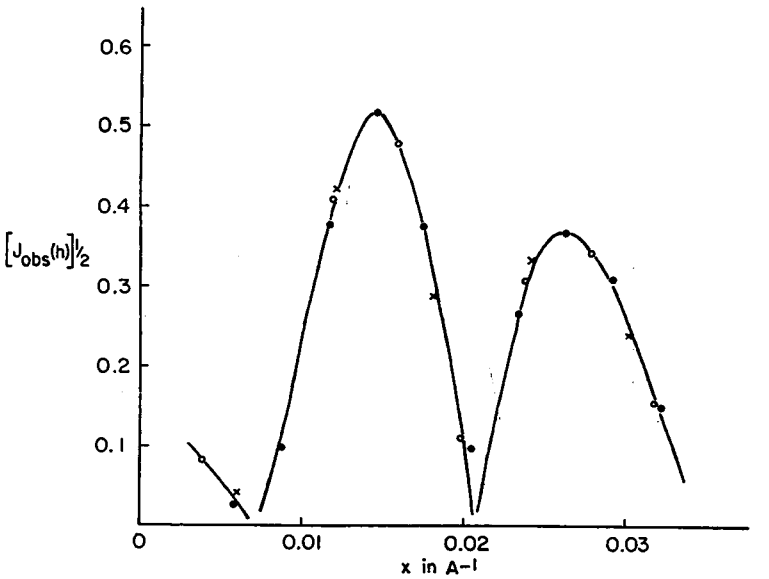

FIGURE 2 The modulus of the amplitude $[J_{obs}(h)]^{1/2}$ for three sets of low-angle X-ray data are plotted against X, the reciprocal space coordinate. The three sets of data have been put on the same relative scale using equation 3 *b*. The continuous curve is fitted by eye to the experimental points. (Solid circle) the distilled water data, $d = 342$ A; (open circle) the distilled water data, $d = 252$ A; (cross) the subnormal nerve data, $d = 166$ A.

intensity data to the same relative scale is likely to be correct. This conclusion is also supported by the two sets of intensity data from frog sciatic nerve swollen in distilled water, and we also note that the intensity data from a subnormal pattern of nerve myelin lies on the same continuous curve.

DERIVATION OF A MODEL

The model approach requires one to first choose a possible model. In electron micrographs, for example, those shown by Robertson (1964), the Schwann cell membranes show the familiar triple-layered membrane unit, whereas, electron micrographs of nerve myelin generally show a dense line corresponding to the two cytoplasmic Schwann cell membrane surfaces and an intraperiod line corresponding to the two extracellular Schwann cell membranes. This then suggests some structural difference between the cytoplasmic and extracellular surfaces, but this difference is not apparent in electron micrographs before myelination. The choice of a model for nerve myelin is therefore not obvious.

We choose the familiar triple-layered unit as a model for the Schwann cell membrane, let them touch at their cytoplasmic surfaces but leave an interspace between the extracellular surfaces. This model for nerve myelin does not account for the dense and intraperiod lines seen in the electron micrographs, but we examine this model nevertheless.

The familiar triple-layered membrane unit is thought to consist of a layer of lipid with the surfaces covered by a layer of nonlipid or protein. However, we have in mind a model which refers specifically to electron densities rather than to chemical composition. Let the central layer have thickness l and electron density L and the outer surfaces have thickness p and electron densities P. The radial repeat distance is d and there are two triple-layered units per radial repeat. The width of a membrane pair is $w = 2(2p + l)$ and this leaves an interspace of width $d - w$ which contains fluid of electron density F. The model is centrosymmetric. There are five model parameters l, w, P, L, and F. This centrosymmetric model is shown in Fig. 3.

In order to test whether this model might be in agreement with the low-angle data, the Fourier transform of the model $T(X)$ is required. We write the Fourier transform $T(X)$ as $T(X) = T(0) + T'(X)$, as only $T'(X)$ is needed for we want to compare $T'(X)$, $X = h/d$ with the low-angle X-ray data $J_{obs}(h)$, that is, via $[J_{obs}(h)]^{1/2}$. The Fourier tranform $T'(X)$ for the model shown in Fig. 3 has been derived, (see $T'(X)$ for model (2 d) in Table II, Worthington, 1969). We express $T'(X)$ in a more convenient form

$$T'(X) = (P - F)w \operatorname{sinc} \pi wX - 2(P - L)l \operatorname{sinc} \pi lX \cos \pi wX/2, \qquad (4)$$

where $\operatorname{sinc} \theta = \sin \theta/\theta$.

Consider a set of intensities $J_{obs}(h)$ obtained from a typical swollen pattern of peripheral nerve myelin, in particular, the low-angle X-ray diffraction pattern of frog

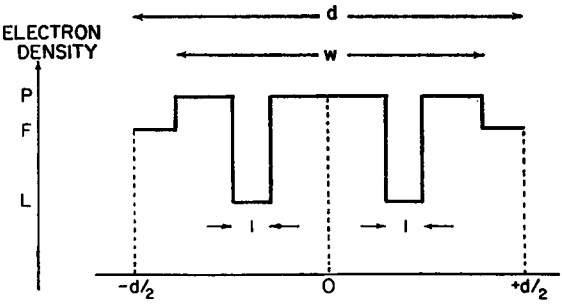

FIGURE 3 The model of nerve myelin is centrosymmetrical and has repeat distance d and membrane pair thickness w. The electron density scale is shown on the left.

sciatic nerve in distilled water which shows eight order of $d = 252$ A. A plot of the amplitude (modulus) $[J_{obs}(h)]^{1/2}$ against the reciprocal space coordinate X is shown in Fig. 2. A continuous curve connects the experimental points and defines regions I, II, and III. The minima can be drawn in fairly readily; all swollen patterns of nerve show the same three regions and the minima occur approximately in the ratio of 1:3:5. The peak intensity of region II generally exceeds that of region III in swollen patterns of nerve.

The first term in equation 4 is zero when sinc $\pi wX = 0$, that is, when $X = m/w$, m is any integer except zero. The second term in equation 4 is zero when cos $(\pi/2)wX = 0$, that is, when $X = n/w$, n is an odd integer. Hence, it follows that $T'(X)$ in equation 4 has zeroes at $X = n/w$, n odd and the first three zeroes occur precisely at $X = 1/w$, $3/w$, and $5/w$. This feature is also shown to a good approximation by the experimental $[J_{obs}(h)]^{1/2}$ curve in Fig. 2 and a value for w can be directly assigned. The peak intensity of region II occurs at close to $X \approx 2/w$ and that of region III occurs at close to $x \approx 4/w$. If we denote the ratio of the peak intensity in region II to that of the peak intensity in region III as θ^2 then from equation 4 the magnitude of this ratio is governed by the term sin π lX, that is, governed by the magnitude of l. It follows that cos 2π $l/w \approx 1/\theta$ and hence there are two values of l which have the same intensity ratio.

In the above we have identified parameters l, w with characteristic features of the amplitude (modulus) plot shown in Fig. 2. However, altogether there are five parameters l, w, P, L, F, and each parameter influences the shape of the Fourier transform $T'(X)$. Before giving a description of the model parameters, we first examine the various kinds of possible models which can give some measure of agreement with our experimental data $J_{obs}(h)$.

PHASE PROBLEM OF SWOLLEN PERIPHERAL NERVE MYELIN

A description of the phase problem of swollen peripheral nerve myelin can be given in terms of the model shown in Fig. 3. As we assume that the radial repeating unit

contains a center of symmetry, the phase of each region can be either + or −. Therefore, there are eight possible sets of phases within the three regions, these are ±, ±, ±. By assigning different parameters to the model shown in Fig. 3, we find that there are eight possible kinds of models to consider, one for each set of phases. We have assumed $P > L$, that is, the lower electron density is placed within the central region of the Schwann cell membrane. This eliminates half of the possibilities and leaves four possible sets of phases which are ±, +, ±. The phases in region I depend on the size of the average membrane pair electron density M compared to the electron density within the fluid layer F, where, in terms of the model shown in Fig. 3, M is given by

$$M = (4pP + 2lL)/w. \tag{5}$$

In region I the Fourier transform $T'(X)$ defined in equation 4 can be approximated by

$$T'(X) = (M - F)w \text{ sinc } \pi wX \tag{6}$$

where sinc θ = sin θ/θ, provided that only very small angles of diffraction are considered (Worthington, 1969). Therefore, in terms of our model a+ phase in region I corresponds to $M > F$ whereas a− phase corresponds to $M < F$. We have previously noted there are two values of l which give the same $J'(X)$ at $X \approx 2/w$ and $X \approx 4/w$. A small value of l corresponds to a− phase in region III whereas a large value of l corresponds to a+ phase in region III. In order to reduce the number of possible models to two, we need to know the magnitude of the average electron density of the membrane pair.

DETERMINATION OF MODEL PARAMETERS

We assume that the electron density of the fluid layer F is the same as the medium in which the nerve fiber is immersed, and hence F is known. This leaves four parameters l, w, P, and L. There are eight kinds of models to consider, one for each set of phases. If $P > L$ then the choice of L in the central region of the Schwann cell membrane reduces the possibilities to four kinds of models. We have noted in the derivation of a model section that the width w is fixed by the intensity minima and the central region width l can have two possible values. The four kinds of models are as follows:

I $M - F > 0$, l small;
II $M - F < 0$, l small;
III $M - F > 0$, l large;
IV $M - F < 0$, l large.

Anyone of these four kinds of models can have a whole series of values for P and L

but they are related by equation 5. In an earlier report (Worthington and Blaurock, 1968) the results of model calculations using only specific values for P and L were described. We now examine all possible combinations of P and L and thus we write $P - F = \alpha(P - L)$, where α is a ratio, so that $T'(X)$ in equation 4 becomes

$$T'(X) = (P - L)[\alpha w \operatorname{sinc} \pi wX - 2l \operatorname{sinc} \pi lX \cos \pi wX/2]. \quad (7)$$

The $T'(h)$ values calculated from a model with parameters l, w, P, L, F, are compared with the low-angle X-ray diffraction data and the agreement is measured by the R-value. However, in computing the R-value the $(P - L)$ term in equation 7 is eliminated in the normalization procedure. Hence, as we assume knowledge of F, we can search for a minimum R-value by varying the model parameters l, w, α. The R-values for the four kinds of models are shown in Table III for the three sets of data from swollen nerve.

From Table III we note the following: models I and II have approximately the same l, w with l small and models III and IV have approximately the same l, w with l large. Only models I and/or II give good agreement with the low-angle X-ray data. On the other hand, models III and IV give poor agreement with the low-angle X-ray data, and hence the kind of model which has a large central region of comparatively low uniform electron density is not in agreement with the intensity data from swollen peripheral nerve myelin. Therefore, the Schwann cell membrane in swollen nerve does not contain an extended lipid bilayer (that is, an extended bilayer which has a uniform region of low electron density) but contains only a narrow region of low uniform electron density. We delay any choice between models I and II until an estimation of the actual value of the average electron density of membrane pair (M) has been obtained.

In assigning model parameters to the intact nerves and to subnormal peripheral

TABLE III

MODEL PARAMETERS l, w, α FOR SWOLLEN NERVE

(1) Frog sicatic nerve in distilled water, d = 252 A
model I, w = 145 A, l = 17.5 A, α = 0.34 and R = 10%
model II, w = 145 A, l = 18.0 A, α = 0.22 and R = 7%.
model III, w = 142 A, l = 51.0 A, α = 0.84 and R = 32%.
model IV, w = 142 A, l = 52.0 A, α = 0.70 and R = 33%.
(2) Frog sciatic nerve in 0.24 M sucrose solution, d = 388 A.
model I and II, w = 142 A, l = 21.0 A, α = 0.28 and R = 6%.
model III, w = 141 A, l = 49.0 A, α = 0.74 and R = 29%.
model IV, w = 140 A, l = 48.0 A, α = 0.68 and R = 29%.
(3) Frog sciatic nerve in 0.83 M sucrose solution, d = 359 A.
model I, w = 142 A, l = 27.0 A, α = 0.58 and R = 34%.
model II, w = 140 A, l = 27.5 A, α = 0.16 and R = 9%.
model III, w = 143 A, l = 43.0 A, α = 0.80 and R = 36%.
model IV, w = 140 A, l = 41.5 A, α = 0.43 and R = 21%.

nerve we can reject models III and IV but again we have difficulty in deciding between models I and II. The reason for this is that these patterns have only one order of diffraction in region I and, furthermore, this reflection has weak intensity as it occurs relatively close to the first minima of the transform $T'(X)$. We also note that, in the case of intact nerve, $M \approx F$ and hence the transform $T'(X)$ will be comparatively small within region I. In our determination of model parameters we can only find one R-value minimum, this may consist of two overlapping minima belonging to models I and II. We list the model parameters l, w for the various intact nerves in Table III. Parameters were obtained by computing the R-value using the first six orders of diffraction for peripheral nerve myelin and the first five orders of diffraction for the central nervous system myelin.

From Table IV the agreement for the intact peripheral nerves $R \approx 11$ to 14 % is not as good as the swollen nerves in Table III where $R \approx 7$ to 9 %. The low-angle X-ray data for the intact peripheral nerves includes one reflection outside region III but has a reciprocal spacing cut-off $X_o \approx 3.5 \times 10^{-2}$ A^{-1} which is not very different from that of the swollen nerves (see Figs. 1 and 2). Hence some modification to the model shown in Fig. 3 is needed in order to give better agreement with observed X-ray data. This leads to additional model parameters but meaningful parameters can only be obtained using a diffraction pattern of nerve which shows more than six orders of diffraction. This more complex model building may be possible in future work.

From Table IV the agreement for the central nervous system intact nerves is quite good. The R-value was computed using only the first five orders of diffraction but the reciprocal space cut-off values $X_o \approx 3.1$ to 3.3×10^{-2} A^{-1} are only slightly less than those for the peripheral nerve data.

Model parameters can be assigned to the sub-normal pattern obtained from immersing frog sciatic nerve, pre-swollen in distilled water, in 1 mM $CaCl_2$ solution. The model parameters were obtained as the result of computing the R-value using the first seven orders of the subnormal pattern $d = 166$ A. The parameters are as follows $w = 145.5$ A, $l = 18.0$ A with $R = 10$ %; compare $w = 145.0$ A, $l = 17.5$ A with $R = 10$ % for the distilled water data. The dimensions (l, w) of the membrane pair have been obtained for frog sciatic nerve in three different states: the normal

TABLE IV

MODEL PARAMETERS l, w FOR INTACT NERVE MYELIN

(1) Peripheral nerve myelin							
frog sciatic nerve,	d = 171 A,	w = 155 A,	l = 19.5 A and	R = 11%
rat sciatic nerve,	d = 176 A,	w = 157.5 A,	l = 16.0 A and	R = 14%.
chicken sciatic nerve,	d = 182 A,	w = 166 A,	l = 19.0 A and	R = 12%.
(2) Central nervous system myelin							
frog optic nerve,	d = 154 A,	w = 146 A,	l = 21.0 A and	R = 7%.
rat optic nerve,	d = 159 A,	w = 150.5 A,	l = 21.5 A and	R = 9%.
chicken optic nerve,	d = 155 A,	w = 148.5 A,	l = 24.5 A and	R = 7%.
frog spinal cord,	d = 153 A,	w = 144 A,	l = 20.0 A and	R = 6%.

state, the swollen state (consider the distilled water case), and the subnormal state. The dimension are $w \approx 145$ A, $l \approx 18$ A for the swollen and subnormal states but $w \approx 155$ A, $l \approx 20$ A for the normal state. Our observation that the membrane pair dimensions are about the same for the swollen and subnormal states could also have been anticipated to some extent from an inspection of Fig. 2. The intensity data from the subnormal pattern lie on the intensity curve of nerve swollen in distilled water.

THE PATTERSON FUNCTION

The Patterson function requires no phase information and can be directly calculated. The Patterson function $P''(x)$ uses the observed intensity data $J_{obs}(h)$ and is given by

$$P''(x) = (2/d) \sum_{1}^{h} J_{obs}(h) \cos 2\pi hx/d. \tag{8}$$

An interpretation of $P''(x)$ obtained from biological tissue in terms of structure is usually not possible. However, in the special case of swollen nerve, characteristic features in $P''(x)$ can sometimes be identified with parameters of a model (Worthington, 1969). Patterson functions of peripheral nerve myelin have been published by Finean (1960), but these contain the integrated intensity $I(h)$ instead of $J_{obs}(h)$ as used in equation 8 and hence these earlier Patterson functions differ from ours. For instance, the Patterson function for normal peripheral nerve myelin (Finean, 1960) shows a strong peak at $d/2$ and a minor peak at $d/4$, the Patterson function for intact frog sciatic nerve computed from equation 8 and using the first five orders of diffraction shows the same two peaks at $d/2$ and at $d/4$ but the shape of the peaks including that of the origin is essentially different. An interpretation of the earlier Patterson function for normal nerve myelin (Finean, 1960) has not been given. Before providing an interpretation of the Patterson function for intact frog sciatic nerve (to be described) it is instructive to examine the Patterson function for swollen nerve.

The Patterson function $P''(x)$ for frog sciatic nerve swollen in distilled water using the data from Table I is shown in Fig. 4. There is a strong peak at $x = 72.5$ A and its height is approximately one-half that of the origin peak. Both the origin and the strong peak have a fall-off which ends at a distance of about 23–24 A from the center of the peaks. A minor peak is discernible at $x \approx 45$ A.

The Patterson function of the model shown in Fig. 3 has been derived and its characteristic features identified with the parameters of the model (Worthington, 1969). If $d \geqq 2w$, then the Patterson function calculated from the model has the following features. A strong peak occurs at $x = w/2$ and has a height one-half that of the origin, the origin and strong peak fall-off ends at $x = l$ and a minor peak occurs at $x = p + l$. If $d < 2w$ then the above theory only applies in the range $0 \leqq x \leqq d - w$, outside this range the theory is an approximation. In the case of peripheral

nerve swollen in distilled water, $d - w = 107$ A, and we can apply the above theory from $x = 0$ to $x = 107$ A. In Fig. 4 $P''(x)$ shows a strong peak which has a height one-half that of the origin, and we can assign $w \approx 144$–145 A. The parameter l is obtained from the location of the origin and strong peak fall-off, this gives $l \approx 23$–24 A, but because of the limited resolution in $P''(x)$, a better estimate is obtained by extrapolating the straight portion of the curve which gives $l \approx 20$ A. The minor peak occurs at $p + l \approx 42$ A. From Table III the model parameters for the same nerve are $w = 145$ A, $l = 17.5$ A and $p + l = 45$ A. The agreement with the width of the membrane pair is excellent; the strong peak is fairly well defined in $P''(x)$ and this leads to a fairly precise value. From Table III we note that models III and IV have $w = 142$ A which is not shown by $P''(x)$. The agreement with the width of the central region of low electron density is fairly good but we have the problem of allowing for the limited resolution of $P''(x)$ in estimating l. The minor peak is not well defined and our estimation of $p + l$ is 3 A less than that given by the model.

The Patterson function $P''(x)$ of intact frog sciatic nerve computed using the first five orders of diffraction is shown in Fig. 5. The interpretation of the intact nerve $P''(x)$, where $d \gtrsim w$, is not as simple as the swollen case, but the theory is exact for $0 \leqq x \leqq d - w$ and only approximate for the remaining values of x. We apply this approximate theory. From Fig. 5 the following features are noted. The origin fall-off ends at 24 A, if we extrapolate the straight portion of the curve then this occurs at 20 A, so that $l \approx 20$ A. A strong peak occurs at $d/2$ and a well defined minor peak occurs at $d/4$. From Table IV the model parameters for intact frog sciatic nerve are $w = 155$ A, $l = 19.5$ A with $p + l = 48.5$ A. The agreement with l

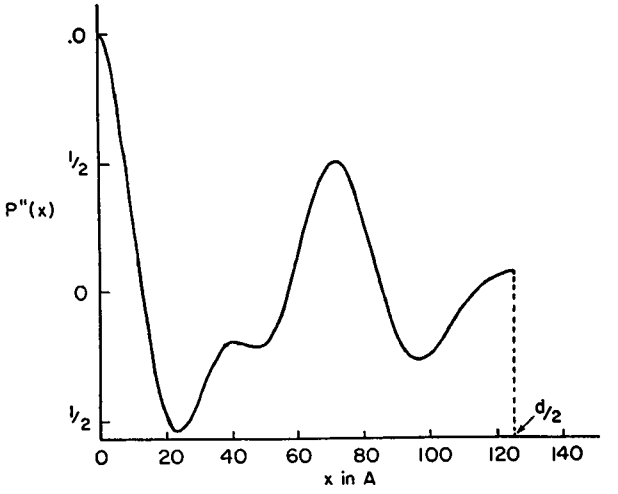

FIGURE 4 The Patterson function for frog sciatic nerve swollen in distilled water $d = 252$ A. The Patterson function was computed using equation 8 and intensity data $J_{obs}(h)$ given in Table I.

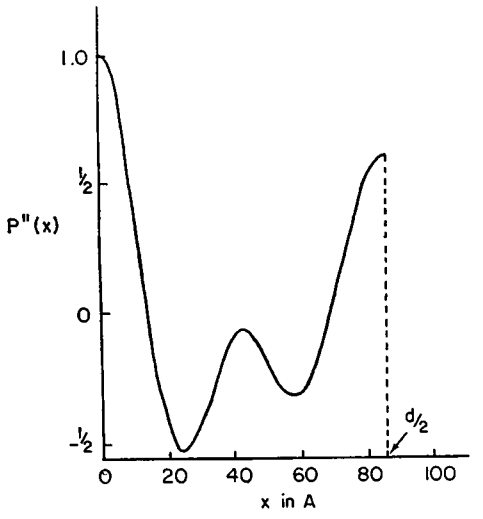

FIGURE 5 The Patterson function for intact frog sciatic nerve d = 171 A. The Patterson function was computed using equation 8 and the first five intensity values $J_{obs}(h)$ given in Table I.

is reasonable. At first sight we might assign $w = d/2$ but from Fig. 5 we see that the fall-off of this peak ends at a distance 29 A from $d/2$ instead of the expected distance 24 A. This suggests that the peak at $d/2$ consists of two overlapping peaks but appears single because of the limited resolution of $P''(x)$. By plotting two origin peaks at a distance of 8 A on either side of $d/2$ and, by addition, a single peak is obtained which is identical in shape to that shown in Fig. 5. Hence, we deduce that the peak at $d/2$ is double and consists of two peaks separated by a distance of 16 A, the first strong peak then occurs at x = 77.5 A in agreement with the model parameter w = 155 A obtained by computing the R-value. The minor peak is at $d/4$ = 43 A and is less than the model value by 5.5 A. The interpretation of the minor peak is not entirely satisfactory and a more sophisticated model is needed to give better agreement.[1]

In summary a study of the Patterson function $P''(x)$ can lead to the assignment of the model parameters l, w in the swollen case ($d \gtrsim 2w$). This also holds for the 0.24 and 0.82 M data, $P''(x)$ for these two data sets is not shown, but is similar to that for the water data except that the minor peak is poorly developed. In the normal case ($d \gtrsim w$) a study of $P''(x)$ can lead to an assignment of l, w but the assignment of l is indirect. However, we note that the Patterson function $P''(x)$ has limited resolution and the model parameters are obtained more precisely by computing the R-values as in the previous section.

DETERMINATION OF M FOR SWOLLEN PERIPHERAL NERVE

From Figs. 1 and 2 we see that in regions II and III the continuous curves have similar magnitudes and shapes for the l, w parameters are not very different. Differ-

[1] See Note Added in Proof at end of article.

ences are apparent in region I, these differences mainly reflect the differences between the average electron density of the membrane pair M and that of the fluid layer F, that is, $M - F$. If we examine the $J_{obs}(h)$ values for the three sets of data from swollen nerve within region I, the $J_{obs}(h)$ values given in Table I are on the same relative scale, then we see that $J_{obs}(h)$ for the 0.82 M data exceeds $J_{obs}(h)$ for distilled water, whereas, the $J_{obs}(h)$ values for 0.24 M sucrose are the smallest and, in fact, are almost zero. The electron densities for distilled water, 0.24 and 0.82 M sucrose solutions are 0.334, 0.343 and 0.366 electrons/A^3 respectively. From equation 6 in the case of nerve in 0.24 M sucrose solution we have $M \approx F$, that is, $M \approx 0.343$ electrons/A^3.

A value for M can also be found by analyzing the distilled water and 0.82 M sucrose data in region I provided that we assume M is the same for both sets of data. The $J_{obs}(h)$ data for distilled water and 0.82 M sucrose is shown in Fig. 6, where we choose to plot the amplitude modulus $[J_{obs}(h)]^{1/2}$. There are two distilled water experimental points, these come from two different sets of data, $d = 252$ A and $d = 342$ A which are shown in Fig. 2. There are two experimental points for the 0.82 M data. In order to draw in a better curve zeroes are included at $X = 1/w$ using the w values given in Table III. For any value of X within region I, the amplitude ratio (A.R.) of the two curves is given by A.R. $\approx (0.366 - M):(M - 0.334)$. If $M = 0.344$, 0.343, 0.342 electrons/A^3 then the corresponding A.R. values are 2.19, 2.54, and 3.00. From Fig. 6, by making measurements within the region of X from 2×10^{-2} to 4×10^{-2} A^{-1}, an A.R. of 2.5 is obtained. Hence, we assign a value of 0.343 electrons/A^3 to the average electron density of the membrane pair.

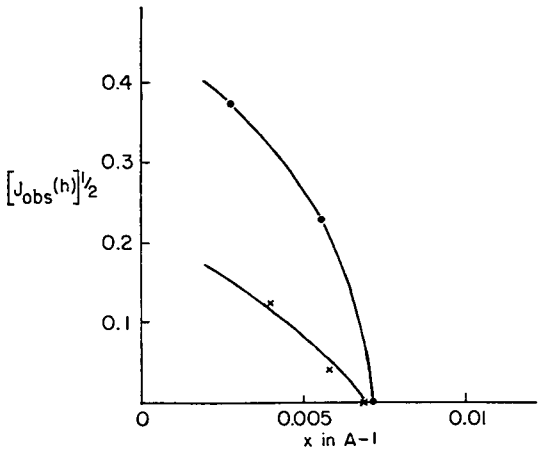

FIGURE 6 The modulus of the amplitude $[J_{obs}(h)]^{1/2}$ for two sets of low-angle X-ray data are plotted in region I against X, the reciprocal space coordinate. The data are on the same relative scale via equation 3 *b*. (Solid circle) the 0.82 M sucrose data, $d = 359$ A; (cross) the distilled water data, $d = 252$A and $d = 342$ A.

The present determination of M follows from our interpretation of the two sets of intensities recorded at fairly small angles of diffraction. Our value is consistent with that deduced from the 0.24 M sucrose data. Realistically, we note that our determination of $M = 0.343$ electrons/A^3 is subject to possible errors. For instance, the data sets are not extensive in region I and comparison between different sets has been made by using equation 3*b*. Also, our assumption that M is a constant for our swollen nerve data can be criticized on the grounds that a small change in the thickness of the membrane pair occurs with an increase in sucrose concentration. Nevertheless, we make use of this value in the next section.

ELECTRON DENSITY LEVELS IN SWOLLEN PERIPHERAL NERVE

The electron density levels P and L in swollen peripheral nerve are related to the term $M - F$ as follows. There are two expressions for $T'(X)$, equations 6 and 7. If we combine equations 6 and 7 and in the limit $X \to 0$ we obtain

$$(M - F)w = (P - L)(\alpha w - 2l) \tag{9}$$

where M and $P - L$ are the unknown quantities. We have three sets of data to consider, frog sciatic nerve swollen in distilled water, 0.24 and 0.82 M sucrose solutions. Each set of data has a different set of parameters l, w, and hence the electron densities of the membrane pair M, P, and L are likely to differ in each of the three cases. Therefore, application of equation 9 to the three data sets leads to no unique solution for either M or $P - L$ because each equation contains two unknown quantities. However, if we assume that M is constant for each of the three cases, on substituting our value of $M = 0.343$ electrons/A^3 and using the values for l, w given in Table III, we obtain the following three equations:

$$(0.343 - 0.334)145 = (P - L)(+14) \tag{10}$$

$$(0.343 - 0.343)142 = (P - L)(-1) \tag{11}$$

$$(0.343 - 0.366)140 = (P - L)(-33). \tag{12}$$

Equation 11 cannot be relied upon as $M - F$ approaches zero and, in any case, the correct value of α is not known. The α value in equation 11 refers to model II but a choice between models I and II has not been made. Equation 10 gives $P - L = 0.093$ electrons/A^3 and equation 12 gives $P - L = 0.098$ electrons/A^3. In the case of the 0.24 M sucrose data, by interpolating between these values, we estimate that $P - L \approx 0.095$ electrons/A^3.

Knowledge of $P - L$ and α provides a determination of P and L: $P =$

$F + \alpha(P - L)$ and L follows at once. The following values of P and L are obtained:

nerve swollen in distilled water, $P = 0.368$ and $L = 0.275$ electrons/A^3;

nerve swollen in 0.24 M sucrose, $P = 0.370$ and $L = 0.274$ electrons/A^3;

nerve swollen in 0.82 M sucrose, $P = 0.382$ and $L = 0.284$ electrons/A^3.

SOLUTION TO THE PHASE PROBLEM OF SWOLLEN PERIPHERAL NERVE

If, for argument sake, we consider the three sets of intensity data from swollen nerve as totally unrelated sets of data, then we would have difficulty in deciding between models I and II. In the case of the water data, model II has a lower R-value than model I, in the case of the 0.24 M data, a choice between models I and II is not possible as the R-value minima overlap, but for the 0.82 M data, model II is clearly favored. However, we have estimated that M = 0.343 electrons/A^3 and therefore model I is the correct choice for the distilled water data, model II is the correct choice for the 0.82 M sucrose data, but in the case of the 0.24 M sucrose data, a choice between models I and II is not possible as the two R-value minima overlap. The phases for peripheral nerve swollen in distilled water for regions I, II and III are +, +, −. The phases for peripheral nerve swollen in 0.82 M sucrose for regions I, II and III are −, +, −.

COMMENT ON THE PHASE PROBLEM OF INTACT NERVE

In the case of the intact nerves (and also the subnormal peripheral nerve pattern) we have noted that it was not possible to decide between models I and II because only one R-value minima was found in the vicinity of $0 \leqq \alpha \leqq \frac{1}{2}$. This was at $\alpha \approx 0.20$ and is associated with model II. We have noted that in deriving possible models to fit the low-angle X-ray data from nerve swollen in distilled water, the model which gives the best fit is not necessarily the correct one. A choice has been made by a comparison with three sets of data from swollen nerve. Therefore, in the case of the intact nerves, we cannot immediately choose model II over model I until model I has been fully examined. From our estimation of $M = 0.343$ electrons/A^3 for swollen nerve, it can be extrapolated that M for intact nerve would be slightly less than this value because w has increased slightly. If we assume that F has an electron density which is about the same as in Ringer's solution, that is, $F \approx 0.338$ electrons/A^3, then $M - F$ is small but positive. A study of equation 7 in region I shows that, if $M - F$ is small and positive, then $T'(X)$ which is positive for $X \to 0$ will change sign in the vicinity of the first minima of region I. Therefore, we can provisionally assign the following phases to the first five orders of diffraction from intact nerve; these are −, +, +, −, −.

This assignment of phases is valid for either peripheral nerve myelin or central

nervous system myelin. Phases for the first five orders of peripheral nerve myelin have been described. Finean (1962) computed a Fourier synthesis using the set +, +, +, −, − but Finean and Burge (1963) later used the set −, +, +, −, −. Moody (1963) could not decide on the sign of the first order but gave +, +, −, − phases for the next four orders of diffraction. We confirm the difficulty in assigning a phase to the first order of diffraction from intact nerve.

DISCUSSION

The present structure analysis has been primarily aimed at deriving an electron density strip model for swollen peripheral nerve myelin. If we assume that the electron density of the membrane pair does not change when immersed in three concentrations of sucrose solutions (0, 0.24, and 0.82 M sucrose), then an estimation of $M = 0.343$ electrons/A^3 is obtained. This estimation of M together with R-value calculations lead to an assignment of models for nerve swollen in distilled water and 0.82 M sucrose, but for nerve swollen in 0.24 M sucrose there is a choice between two models. It follows that the phases in regions I, II, and III are known for nerve swollen in distilled water and 0.82 M sucrose, but only the phases in regions II and III are known for nerve swollen in 0.24 M sucrose.

Our analysis leads to a description of electron densities P and L in the membrane pair of swollen nerve. We find that the electron density of the central region is 0.274–0.284 electrons/A^3. This comparatively low value of electron density is identifiable with the hydrocarbon region of the lipid molecules. In particular, we note that our electron density values for L fall within the range of electron densities for lipid molecules in the liquid state. For instance, the electron densities of saturated and mono-unsaturated liquid n-hydrocarbons (computed from densities in the Handbook of Chemistry and Physics, 46th edition) range from 0.25 to 0.29 electrons/A^3. A crystalline array of hydrocarbon chains will have a somewhat higher electron density. Chapman (1965) in a survey of X-ray studies on lipid crystals gives the volume occupied per CH_2 molecule for a series of lipids, the corresponding electron densities range from 0.32 to 0.35 electrons/A^3. If we assume that the lipid hydrocarbon chains occur in the central region, then it follows that the outer regions of width p contain the non-lipid molecules (20% by dry weight) and the head groups of the lipid molecules plus an unknown amount of fluid. The electron density values for P of 0.365–0.384 electrons/A^3 are not unreasonable for the contents of the outer region.

We note that the resolution Δx of our low-angle X-ray diffraction data, that is, the resolution of a Fourier series representation or a Patterson function, computed using this data, is given by $\Delta x = \frac{1}{2}\,(X_o^{-1})$ and $\Delta x \approx 17$ A. However the values assigned to the model parameters have a much higher precision, judging from the shape of the R-value minima the model parameters obtained for swollen peripheral nerve are accurate to 1%. We note that w decreases from 145 to 140 A but l increases

from 17.5 to 27.5 A on increasing the sucrose concentration. In the present analysis we have not applied any corrections for thermal vibrations or positional disorder, the application of these corrections would tend to compress the observed range of l but the variation of w would not be changed.

We note that, when the sucrose concentration of the immersion fluid is changed, the dimensions l, w of the membrane pair undergo a definite variation, and therefore the molecular structure of the Schwann cell membrane changes accordingly. This change in membrane parameters is, in some respects, unfortunate for a low-angle X-ray study of the swelling behavior of nerve does not provide low-angle X-ray patterns which can be analyzed in a straight forward manner, that is, the sampling of a unique transform is not obtained. This feature has been noted previously (Worthington and Blaurock, 1969 *b*).

We have previously identified three types of low-angle X-ray patterns shown by peripheral nerve myelin. If we start from a swollen pattern (for instance, frog sciatic nerve in distilled water) then the subnormal pattern is obtained by adding 1 mM $CaCl_2$ and the normal (or intact) pattern is finally obtained after standing for a period of time. The model parameters obtained from the swollen pattern are w = 145 A, l = 17.5 A; the subnormal pattern has w = 145.5 A, l = 18.0 A and the normal pattern has w = 155 A, l = 19.5 A. The membrane parameters do not change appreciably when nerve goes from the swollen state to the subnormal state, but on returning to the normal state, both w and l increase. However, the fluid channel width (d–w) between the extracellular Schwann cell membranes of adjacent membrane pairs shows a decrease of 20.5 A (subnormal) to 16.0 A (normal). Although the molecular structure of the membrane pair of swollen and sub-normal nerve is closely similar, the molecular structure of the membrane pair in normal or intact nerve is essentially different from that of the swollen and the subnormal nerve.

Model parameters have been assigned to a variety of intact peripheral and central nervous system myelins. The low-angle patterns of peripheral nerve myelins show a characteristic intensity variation, and similarly the low-angle patterns of central nervous system myelins show a characteristic intensity variation (Blaurock and Worthington, 1969). The various intact peripheral nerves studied have a variation in d of 171–182 A, the model parameters show some variation, but the largest change occurs in w. We note the width of the fluid channel (d-w) has only a small variation of 16.0–18.5 A. The various intact central nervous system nerves studied have a variation in d of 153–159 A, l has only a small variation as in the case of the peripheral nerves, but w has a moderate variation of 144–150.5 A. However the width of the fluid channel (d-w) has only a small variation of 6.5–9 A.

An interpretation of why peripheral nerve myelin and central nervous system myelin show different intensity variations for the first five order of diffraction can be given. Although the parameters l, w contribute, the dominating factor is the difference in the fluid channel width; the central nervous system channel is about one-half that shown by peripheral nerve myelin. In the case of central nervous system myelin

the X-ray reflections occur close to the reciprocal space values $X = m/w$, m is an integer. Our analysis shows that minima occur at odd values of m and hence the odd orders of diffraction, that is, $h = 1$, 3, and 5 will have weak intensity in agreement with the intensities given in Table II.

In summary, the present structure analysis of nerve myelin shows that a simple triple-layered membrane unit end-to-end but with a single fluid channel per radial repeat is in agreement with the low-angle X-ray data. If we accept this model as being reasonably correct, then there is a narrow hydrocarbon central region in the Schwann cell membrane. Furthermore, if our values for P and L are correct (for swollen nerve) then any proposed model is required to have these values, and this will strongly influence possible ways of packing the molecular components within p and l. Unfortunately, knowledge of these values does not by itself immediately lead to any unique way of assembling the molecular components. For instance, the hydrocarbon chains could be liquid like, in either three or two dimensions, or else crystalline but with certain chains missing in order to account for the estimated low electron density. However, a discussion of the arrangement of hydrocarbon chains in the central regions is better delayed until more evidence is assembled.

Note Added in Proof. A seven parameter model for intact myelinated nerve which is in better agreement with the X-ray data has now been derived. WORTHINGTON, C. R. 1969. *Proc. Nat. Acad. Sci. U.S.A.* In press.

This work was supported by United States Public Health Service Grant GM-09796.

Received for publication 16 January 1969.

REFERENCES

1. BLAUROCK, A. E. and C. R. WORTHINGTON. 1966. *Biophys. J.* **6**:305.
2. BLAUROCK, A. E. and C. R. WORTHINGTON. 1969. *Biochim. Biophys. Acta.* **173**:419.
3. CHAPMAN, D. 1965. The Structure of Lipids. John Wiley & Sons, New York.
4. FINEAN, J. B. 1953. *Experimentia.* **9**:17.
5. FINEAN, J. B. 1960. Modern Scientific Aspects of Neurology. J. N. Cummings, editor. Edward Arnold, Ltd., London, England.
6. FINEAN, J. B. 1962. *Circulation* **26**:1151.
7. FINEAN, J. B., and R. E. BURGE. 1963. *J. Mol. Biol.* **7**:672.
8. FINEAN, J. B., and P. F. MILLINGTON. 1957. *J. Biophys. and Biochem. Cytol.* **3**:89.
9. GEREN, B. B. 1954. *Exp. Cell Res.* **7**:558.
10. MOODY, M. F. 1963. *Science.* **142**:1173.
11. ROBERTSON, J. D. 1964. Cellular Membranes in Development. M. Locke, editor. Academic Press Inc., New York.
12. SCHMITT, F. O., R. S. BEAR, and K. J. PALMER. 1941. *J. Cell. Comp. Physiol.* **18**:31.
13. VANDERHEUVEL, F. A. 1963. *J. Amer. Oil Chem. Soc.* **40**:455.
14. WORTHINGTON, C. R. 1969. *Biophys. J.* **9**:222.
15. WORTHINGTON, C. R., and A. E. BLAUROCK. 1968. *Nature.* **218**:87.
16. WORTHINGTON, C. R., and A. E. BLAUROCK. 1969 *a. Biophys. Soc. Annu. Meet. Abstr.* FAM G13.
17. WORTHINGTON, C. R., and A. E. BLAUROCK. 1969 *b. Biochim. Biophys. Acta.* **173**:427.